International Journal of Pharmaceutics, 14 (1983) 43–58
Elsevier Biomedical Press

Research Papers

Physicochemical characterization of polyacrylic nanoparticles

Jörg Kreuter

Department of Pharmacy, Swiss Federal Institute of Technology (ETH), CH-8092 Zürich (Switzerland)

(Received June 17th, 1982)
(Accepted July 30th, 1982)

Summary

Nanoparticles are polymeric colloidal drug carriers possibly suitable for drug targeting. The physicochemical parameters of polyacrylic nanoparticles, such as the size distribution, specific surface area, density, X-ray diffraction pattern, wettability and surface charge were measured. All polyacrylic nanoparticles had a particle size below 200 nm. They were X-ray amorphous and negatively charged. In serum their surface charge and their water contact angles decreased considerably, indicating a strong interaction with serum components.

Introduction

Nanoparticles are colloidal particles ranging in size from 10 nm to 1000 nm consisting of macromolecular materials in which the active principle is entrapped, encapsulated and/or adsorbed. Due to their colloidal nature, they may be suitable as drug carriers and for drug targeting purposes.

So far their efficacy as adjuvants for vaccines (Kreuter and Speiser, 1976; Kreuter et al., 1976; Kreuter and Liehl, 1978, 1981) and their ability to enhance the anti-tumor activity of certain cytostatic agents has been demonstrated (Brasseur et al., 1980).

For vaccination purposes, the slowly biodegradable poly(methyl methacrylate) nanoparticles is the material of choice (unpublished observation). The slow biodegradability of this material seems to cause a prolonged retention of the antigen which in turn leads to a prolonged immunostimulation. Polycyanoacrylate nanoparticles on the other hand are more suitable for use as drug carriers, because they are rapidly biodegradable.

0378-5173/83/0000–0000/$03.00

Although polyacrylic nanoparticles have been used for several years, very little, and sometimes controversial, information about their physical and physicochemical properties is available. This report attempts to fill in these gaps in information by giving a systematic physicochemical characterization of the presently known polyacrylic nanoparticles.

Materials and methods

Preparation of polyacrylic nanoparticles

Polyacrylamide nanoparticles

Bis-(2-ethylhexyl)sodium sulfosuccinate (12 g) (Fluka, Buchs, Switzerland) and polyoxyethylene-4-lauryl ether (6 g) (Atlas, Essen, F.R.G.) were dissolved in 20 g of *n*-hexane (Fluka). 10 ml of water was added drop by drop under stirring. After addition of a further 20 g of *n*-hexane, 0.25 g of N,N'-methylene-bisacrylamide (CIBA-Geigy, Basel, Switzerland) and 2.0 g acrylamide (CIBA-Geigy) were added and solubilized under stirring. 40 g *n*-hexane was added; nitrogen was bubbled through the solution for 3–5 min with an injection needle to reduce oxygen. Then the solution was irradiated with 300 krad at room temperature in a ^{60}Co-source. Methanol was added to the polymerized nanoparticles so that a methanol–*n*-hexane ratio of 9 : 4 resulted. This mixture was centrifuged (Beckman J 21, Palo Alto, CA) at 0°C with 20,000 *g* for 30 min. The centrifugation pellet containing the nanoparticles was washed 7 times by redispersion and centrifuged in the above methanol–*n*-hexane mixture. Then the nanoparticles were redispersed in water and freeze-dried.

Poly(methyl methacrylate) nanoparticles

Methyl methacrylate (Fluka, Buchs, Switzerland) was purified from polymerization inhibitors as described by Riddle (1954) or Tessmar (1961). The purified monomer was then dissolved in water or in phosphate-buffered saline and polymerized with 500 krad in a ^{60}Co-source at a rate of 2.2 krad/min. The resulting nanoparticle suspension was then used as such or freeze-dried.

Polycyanoacrylate nanoparticles

1% methylcyanoacrylate (Schering, Bergkamen, F.R.G.) ethylcyanoacrylate (Schering) or butylcyanoacrylate (Sichel Werke, Hannover, F.R.G.) was added drop by drop under stirring with a magnetic stirrer to a 0.5% solution of polysorbate 20 (Fluka, Buchs, Switzerland) in 0.1 N hydrochloric acid. This mixture was stirred for 2 h, resulting in the polymerization of the cyanoacrylate and thus forming the nanoparticles. Then this suspension was neutralized with 1 N sodium hydroxide and stirred for an additional 6 h. After this time the nanoparticle suspension was used as such or freeze-dried.

Particle size determination

Scanning electron microscopy

The nanoparticle suspensions were applied to a glass-slide and dried by evaporation of the water at room temperature. After coating with gold, the samples were examined in a Cambridge Stereoscan MARK 2 A (Cambridge Instr., Cambridge, U.K.).

Transmission electron microscopy

The nanoparticle suspensions were applied between two conventional specimen supports for freeze-etching and were frozen using a propane-jet-freezer as described by Müller et al. (1980). The frozen sandwiches were then cleaved in a Balzers BAF 300 freeze-etching apparatus (Balzers AG, Balzers, Liechtenstein) at a temperature of $-165°C$ and a pressure of 2×10^{-7} mbar. Replicas were produced by shadowing with platinum carbon (2 nm) at an angle of 45°. A backing layer of 20 nm of carbon was then applied. The replicas were cleaned with 70% sulfuric acid and a 13% sodium hypochloride solution. Micrographs (Figs. 3–10) were taken in a Philips EM 301 (Philips AG, Eindhoven, Netherlands).

Photon correlation spectrometry

The particle size determination with photon correlation spectrometry was carried out in a K7025 Photon Correlation Spectrometer with 64 channels (Malvern Instr., Malvern, U.K.) equipped with a 14 mW Liconix helium cadmium laser (Liconix, Mountain View, CA, U.S.A.) at 441.6 nm. The nanoparticle suspensions were diluted with water before measurement. The results are shown in Table 1.

Mercury porosimetry

The freeze-dried nanoparticles were filled into a dilatometer under vacuum and then measured in a mercury pressure porosimeter (Carbo Erba AG 60, Milano, Italy). The results are shown in Figs. 1 and 2.

Density

The density of freeze-dried nanoparticles was determined in a Beckman Air Comparison Pycnometer Model 930 (Beckman Instr., Fullerton, CA, U.S.A.) with air and helium. The results are shown in Table 2.

Specific surface area

The specific surface area of freeze-dried nanoparticles was determined with a Perkin-Elmer-Shell Sorptometer (Perkin-Elmer, Norwalk, CT, U.S.A.). The results are shown in Table 4.

X Ray diffraction

The nanoparticle suspensions were applied to the sample holder of a Guinier-De Wolff Camera (Nonius, Netherlands) and the X-ray diffraction was determined (Figs. 11 and 12).

Electrophoretic mobility

The electrophoretic mobility of freeze-dried nanoparticles was determined in a Rank Microelectrophoresis Apparatus Mark II (Rank Bros., Battisham, U.K.) with silver chloride electrodes using white light or a helium gas laser (Scientific and Cook Electr., London, U.K.) as the light source. The polycyanoacrylate nanoparticles were washed prior to the lyophilization 4 times by centrifugation at 121,500 *g* for 1 h 20 min at 10°C in an ultracentrifuge (Sorval OTD 75, Du Pont Instr., Newtown, CT, U.S.A.) and resuspension in water using ultra sonication. In the case of measurement in serum, the samples were stored in this medium overnight. The results are shown in Table 5.

Water contact angle

Freeze-dried nanoparticles were compressed to tablets in a hydraulic laboratory press (Model 340, Apex Constr., London, U.K.). Since no influence of the tableting pressure on the water contact angle was detectable for pressures between 2×10^2 N/cm^2 and 8×10^2 N/cm^2, a pressure of 4×10^2 N/cm^2 was used. Polycyanoacrylate nanoparticles were washed 4 times prior to lyophilization by centrifugation at 121,500 *g* for 1 h 20 min at 10°C in an ultracentrifuge (Sorval OTD 75, Du Pont Instr., Newtown, CT, U.S.A.) and resuspended in water using ultrasonication. Two samples (poly(methyl methacrylate) nanoparticles and polybutylcyanoacrylate nanoparticles), were also stored for 12 h in human serum at 36°C under gentle shaking. Then these samples were centrifuged with 5000 *g* for 15 min. The centrifugation pellet was then freeze-dried and compressed into tablets.

The water contact angles were determined on the tablet surface with a surface wettability tester (Model 2-2, Lorentzen and Wettre, Stockholm, Sweden). In addition, the water contact angle of films made by evaporation of a solution of poly(methyl methacrylate) or polybutylcyanocrylate nanoparticles in acetone were determined. No significant difference was found in comparison to the water contact angle measured on the tablet surfaces of the same material. The results are shown in Table 6.

Results and discussion

Morphology and particle size

The minute particle size is the most characteristic physical parameter of nanoparticles. For this reason, the determination of the particle size is of great importance. However, the sizing in the suboptical size area is associated with considerable difficulties: in this size area the particle size may be altered, or the properties of the materials to be measured may be changed by the sizing procedure. It is also necessary to consider what is actually being measured, especially when dealing with the smaller particles, where hydration or aggregation may have a profound influence on the size of a particle or on the properties of a hydrodynamic layer around the particle.

For the above-outlined reasons, the sizes of different sorts of nanoparticles were

TABLE 1

PARTICLE SIZE OF POLYACRYLIC NANOPARTICLES (MEAN ± S.D)

Polymer type	Sizing method		
	Electron microscope		Photon correlation spectrometry (nm)
	Scanning (nm)	Transmission after freeze-fracturing (nm)	
Poly(methyl methacrylate) [1]	215 ± 44	- *	125 ± 21 **
Poly(methyl methacrylate) [2]	-	-	131 ± 30 **
Polyacrylamide	236 ***	65.7 ± 26.4	52.2 ± 2.1 **
Polymethylcyanoacrylate	- ****	157 ± 98	145 ± 38 **
Polyethylcyanoacrylate	- ****	88.4 ± 14.6	118 ± 34 **
Polybutylcyanoacrylate	- ****	30.9 ± 6.2	51.2 ± 0.7 **

[1] Manufactured by polymerization in pure water.
[2] Manufactured by polymerization in phosphate-buffered saline.
* Not enough particles found.
** Represents standard deviation of measurements, not standard deviation of the particle size distribution.
*** Determined by Kopf (1975).
**** Not determinable because of the surfactant present in the sample.

determined using different methods. The results of these measurements are shown in Table 1.

The results for the nanoparticle sizes found using photon correlation spectrometry and the sizes found with transmission electron microscopy after freeze-fracturing are in very good agreement with each other.

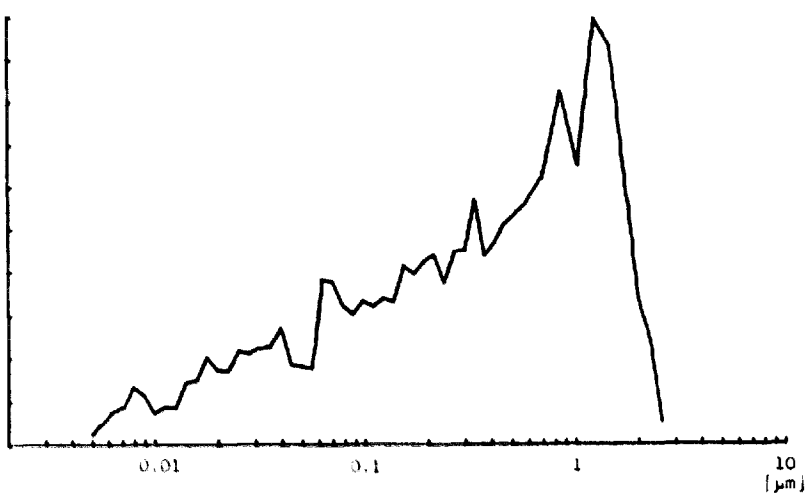

Fig. 1. Size distribution of poly(methyl methacrylate) nanoparticles measured with mercury porosimetry.

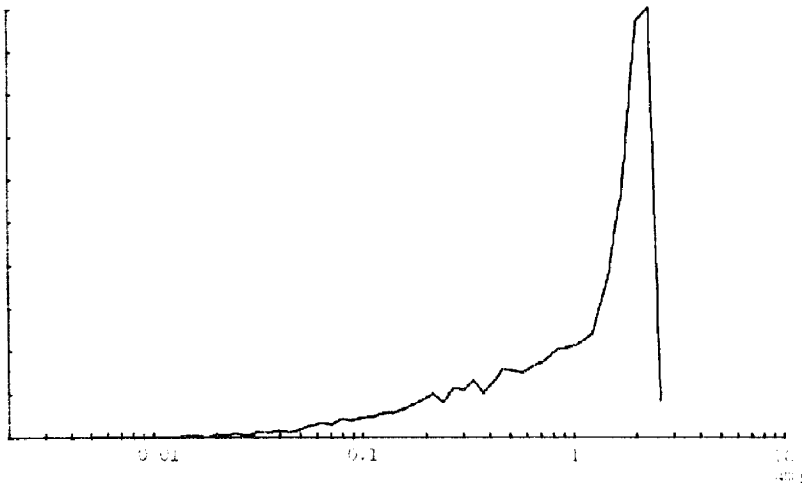

Fig. 2. Size distribution of polyacrylamide nanoparticles measured with mercury porosimetry.

The size of the poly(methyl methacrylate) nanoparticles could not be determined using the freeze-fracturing method because these particles tended to agglomerate before or during the freezing process and therefore too few individual poly(methyl methacrylate) nanoparticles suitable for the size analysis could be found. The size of these particles, however, was well-determined using photon correlation spectrometry after 1 h of sonication. If the sample was left without sonication for 24 h, the poly(methyl methacrylate) nanoparticles started to agglomerate, and the particle size measured with photon correlation spectrometry after this time was about 250 nm. Resonication deglomerated the particles again and the particle size was the same as that obtained after the first sonication of the sample. The particle size shown in Table 1 therefore obviously represents the size of the primary particles.

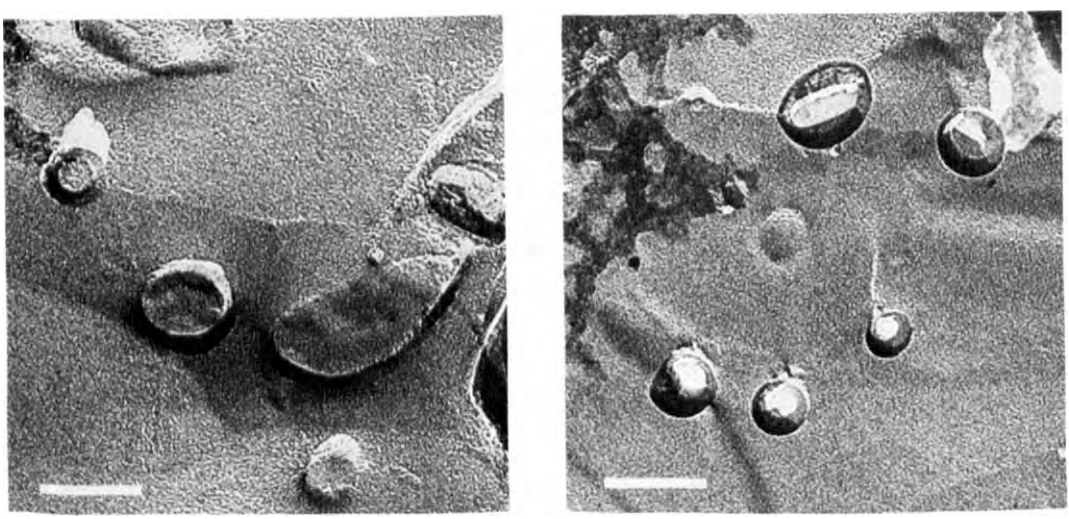

Figs. 3 and 4. Transmission electron micrographs of polyacrylamide nanoparticles after freeze-fracturing. Bar = 100 nm.

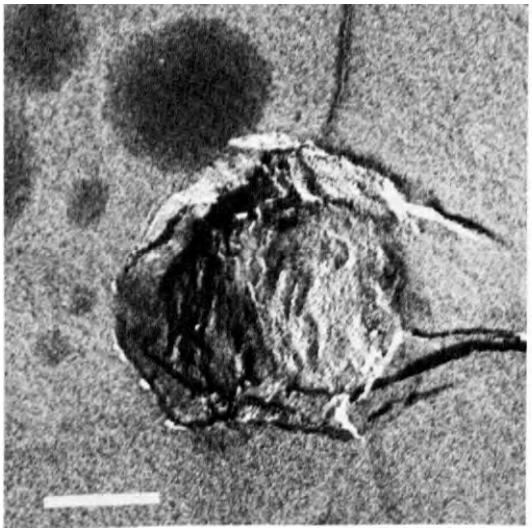

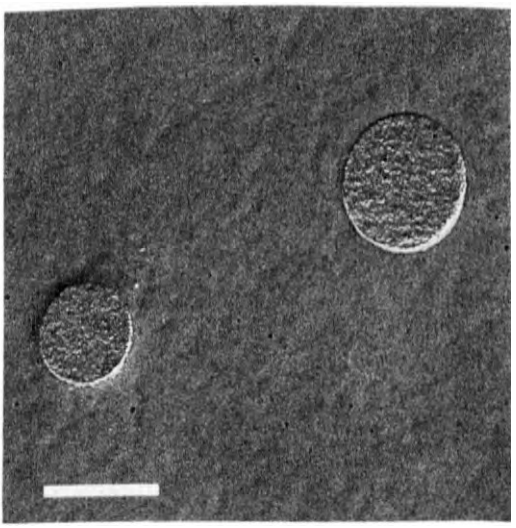

Fig. 5. Transmission electron micrograph of poly(methyl methacrylate) nanoparticles after freeze-fracturing. Bar ≙ 200 nm

Fig. 6. Transmission electron micrograph of polymethylcyanoacrylate nanoparticles after freeze-fracturing. Bar ≙ 200 nm

The results obtained in this study show that photon correlation spectrometry is a very suitable method for the sizing of nanoparticles. However, very disadvantageous is the fact that this method can primarily give the mean diameter. The method provides a polydispersity index; this parameter, however, is only of minor informative value. Multi-modal size distributions cannot be measured. For this reason, photon correlation spectrometry is very susceptible to errors caused by bigger

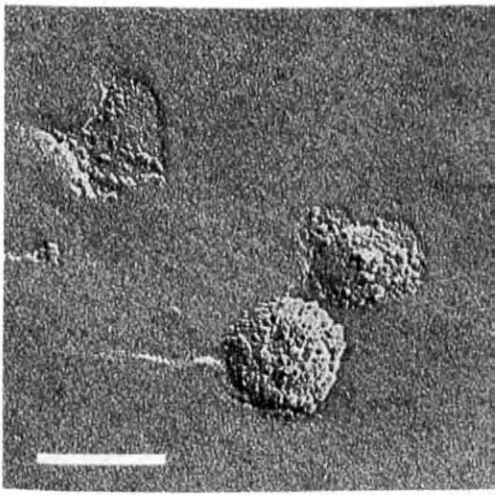

Figs. 7 and 8. Transmission electron micrograph of polyethylcyanoacrylate nanoparticles after freeze-fracturing. Bar ≙ 100 nm

particles that might be present in the samples, such as dust particles or secondary agglomerates. It is therefore necessary that each sample be measured at least 5 times.

Another disadvantage of photon correlation spectrometry can be the fact that this method measures the Brownian motion of the particles. The particle diameter is then calculated from these measurements via the diffusion coefficient. Therefore, the particle size determined using this method will be affected by the influences caused by the surrounding medium such as adsorbed surfactants or by hydration layers and may therefore be different from the particle size determined with other methods such as electron microscopy.

Electron microscopy has the great advantage that individual particles can be analyzed and measured. In addition, freeze-fracturing enables the observation of the interior of the particles and thus enables the investigation of the morphology. The disadvantages of this method are that only very few particles can be observed and that the preparation is extraordinarily time consuming.

Scanning electron microscopy is much less time consuming. However, since the surface of polymers is non-conductive due to their organic nature, the particles have to be coated with gold. The thickness of the gold layer cannot be exactly determined on this type of surface and varies between 30 nm and 60 nm. The size values shown in Table 1 correspond to the gold-coated particles. Since this coat covers the particles on both sides, about 60–120 nm have to be substracted in order to determine the size of the uncoated particles. The particle sizes resulting after substraction are in good agreement with the other size determination methods for poly(methyl methacrylate) nanoparticles and in fair agreement for acrylamide nanoparticles. It has to be considered, that the hard vacuum necessary for electron microscopy as well as the condensing gold can lead to changes in the particle size and may be responsible for the size differences observed for polyacrylamide nanoparticles between scanning electron microscopy and the other techniques. (The

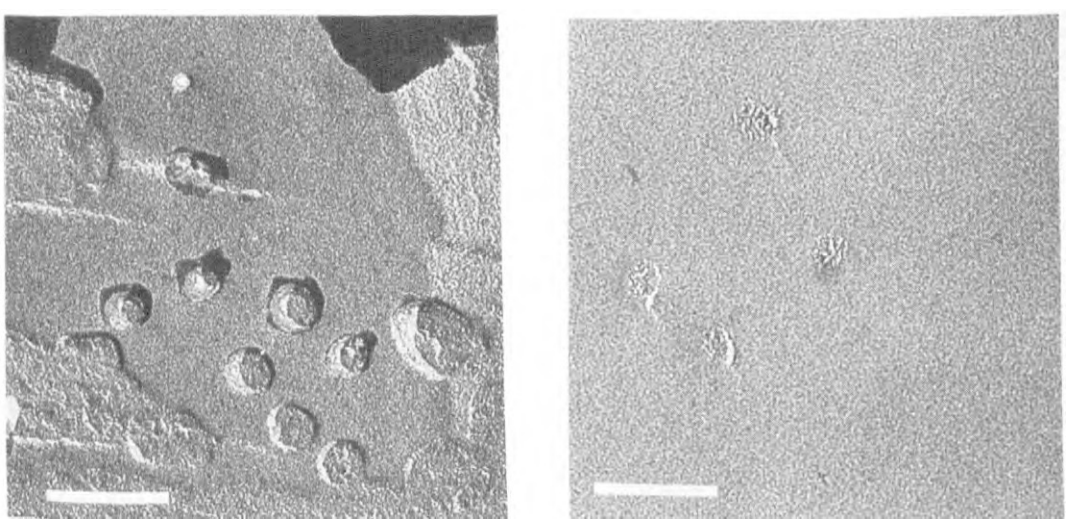

Figs. 9 and 10. Transmission electron micrograph of polybutylcyanoacrylate nanoparticles after freeze-fracturing. Bar ≙ 100 nm.

influence of the hard vacuum is reduced with freeze-fracturing, because the particle is embedded in a supporting medium.)

Scanning electron microscopy cannot be used for the sizing of polycyanoacrylate nanoparticles, because they contain surfactants in their original preparation. The presence of surfactants leads to a smooth coat over the particle surfaces and inhibits the observation of individual structures. This influence of surfactants has already been observed and studied by Kopf (1975; Kopf et al., 1976). Removal of the surfactants, however, often results in aggregation and leads to irreversible changes in the polycyanoacrylate preparations. Therefore, no further attempts were made to visualize them with scanning electron microscopy.

Another method, mercury porosimetry, has been suggested by Mayer and Stowe (1965) for the sizing of small particles. This method was also tested with nanoparticles. The results are shown in Figs. 1 and 2. The particle sizes determined by mercury porosimetry were much larger than those found with other techniques. Mercury porosimetry obviously mainly measures large particle agglomerations. The mercury is not able to penetrate between primary particles to a high degree. This effect has already been observed with fumed silicia (Aerosil 200) (Dr. Kahr, Laboratorium für Grundbau und Bodenmechanik, ETH, Zürich, personal communication). Mercury porosimetry is therefore unsuitable for the sizing of nanoparticles.

The morphology of the polyacrylic nanoparticle preparations was also studied using the transmission electron microscopy after freeze-fracturing. Figs. 3–10 show photos of different individual polyacrylic nanoparticle preparations. All nanoparticles investigated here possess a continuous matrix interior and showed no hollow space as suggested by Birrenbach and Speiser (1976). Certain structures of polyacrylamide particles shown in Fig. 4 that would suggest differences in the density of certain layers in the particle interior or even hollow areas are very probably artefacts caused by the preparation technique. These artefacts occurred because the particles in Fig. 4 were not fractured in the equatorial zone, but broke out of the embedding medium during the freeze-fracturing. This led to the formation of craters in the surrounding medium. The collapse of the crater walls in the vacuum then resulted in different densities of the platinum layer subsequently steamed on the sample, thus creating the above artefact. This assumption can be supported by particles from the same batch shown in Fig. 3. These particles did not break out of the fracturing zone and were fractured through their matrix, thus showing a homogeneous interior.

The polycyanoacrylate and the poly(methyl methacrylate) nanoparticles seem to have an especially porous interior (Figs. 5–10). This has already been observed by Couvreur et al. (1979) with polymethylcyanoacrylate nanoparticles. The polyacrylamide (Figs. 3 and 4) and all polycyanoacrylate nanoparticles (Figs. 6–10) are spherical with a smooth surface. Poly(methyl methacrylate) nanoparticles (Fig. 5) are more irregular, having a rough surface.

Density

The density of poly(methyl methacrylate) and of polyacrylamide nanoparticles is shown in Table 2. The density of the polycyanoacrylate particles could not be determined for the same reason as already mentioned previously. Removal of the

TABLE 2

DENSITY OF POLYACRYLIC NANOPARTICLES

Polymer	Density measured with:	
	Air (g/cm^3)	Helium (g/cm^3)
Poly(methyl methacrylate)	1.40 *	1.06 *
Polyacrylamide	1.30	1.14
Poly(methyl methacrylate) beads ϕ 10 μm	1.15 *	1.15 *

* Literature density of poly(methyl methacrylate) blocks and rods = 1.15–1.8 g/cm^3.

surfactants resulted in an aggregation and clumping of the particles.

The density of poly(methyl methacrylate) nanoparticles was measured with air and helium using a gas pycnometer. The values obtained with air and with helium differ considerably from each other. This effect has already been observed with other materials such as amorphous silicia and activated charcoal (Keng, 1969/70). Table 3 shows that the above-mentioned difference is especially pronounced with substances having a high specific surface area, while no difference was obtained with substances of a low specific surface area such as salt. The reason for the higher values obtained with air is the adsorption of some air components onto the surface of these substances. Therefore, only the essentially non-adsorbing helium should be used for the density measurement of nanoparticles.

Table 2 shows that the density of poly(methyl methacrylate) nanoparticles is considerably lower than that of beads with a diameter of 10 μm or of solid blocks or rods. This result supports our previous observation with the electron microscope after freeze-fracturing and shows that the nanoparticles have a highly porous interior.

The density of polyacrylamide nanoparticles is in good agreement with the reported value by Kopf (1975; Kopf et al., 1976), who determined their density in methanol and in *n*-hexane.

TABLE 3

DENSITY OF SELECTED MATERIALS (FROM KENG, 1969/70)

Material	Density measured with:	
	Air (g/cm^3)	Helium (g/cm^3)
Salt	2.15	2.15
Amorphous silicia, surface area 54.7 m^2/g	2.42	2.11
Amorphous silicia, surface area 295.2 m^2/g	2.85	2.10
Activated charcoal	> 10	2.28

Specific surface area

The specific surface areas of nanoparticles are listed in Table 4. The surface area of poly(methyl methacrylate) and of polyacrylamide nanoparticles was determined using the BET-method as well as by calculation using Eqn. 1:

$$A = \frac{6}{\rho \cdot d} \tag{1}$$

where A is the specific surface area, ρ the density, and d the particle diameter. The measured and the calculated specific surface areas of poly(methyl methacrylate) nanoparticles agree fairly well with each other. In contrast the surface areas of polyacrylamide nanoparticles determined by Kopf (1975; Kopf et al., 1976) with the BET-method are 10 times smaller than the calculated value. This difference can be explained by residual surfactants still present in the samples. Kopf (1975) and Kopf et al. (1976) clearly showed that the surfactants present after the removal of the dispersion medium coat the nanoparticles and lead to the disappearance of individual nanoparticle structures: with higher amounts of surfactants no nanoparticles at all are visible in the scanning electron microscope (Kopf et al., 1976) (Fig. 3). But even the highly purified products (Kopf et al., 1976) (Fig. 1) show considerable amounts of nanoparticle aggregates, probably caused by the coating with residual surfactants. This coating significantly reduces the surface area measurable by nitrogen adsorption and explains the observed difference.

As discussed in the previous sections, polycyanoacrylate nanoparticles so far cannot be obtained surfactant-free in a non-aggregated form. For this reason, no attempts were made to determine the specific surface area of these particles with the BET-method.

TABLE 4

SPECIFIC SURFACE AREA OF NANOPARTICLES

Polymer	Measured by BET-method (m^2/g)	Calculated (m^2/g)
Poly(methyl methacrylate)	52.75 ± 2.26 10 [a]	45.3
Polyacrylamide	8 [b]	100.3
Polymethylcyanoacrylate	– [c]	37.6 [d]
Polyethylcyanoacrylate	– [c]	46.2 [d]
Polybutylcyanoacrylate	– [c]	106.5 [d]

[a] Dried by lyophilization, determined by Kopf (1975).
[b] Dried in vacuum oven, determined by Kopf (1975).
[c] Not determined.
[d] Assumed density 1.1 g/cm^3.

X-Ray diffraction pattern

The X-ray diffraction patterns of polyacrylic nanoparticles are shown in Figs. 11 and 12. All polyacrylic nanoparticles investigated were X-ray amorphous and showed no sign of crystallinity. The X-ray diffraction pattern of poly(methyl methacrylate) beads, diameter 10 μm, is also included in Fig. 11 as a control. These beads are also X-ray amorphous. This shows that the observed differences in density (Table 2) are—unlike in the case of other polymers (Toyoshima, 1973)—not caused by different degrees of crystallinity, but rather by variations in the density of the polymer chain coils.

Electrophoretic mobility

The surface charge of colloidal particles expressed by their electrophoretic mobility seems to have an important influence on their body distribution behaviour in humans and animals (Wilkins and Myers, 1966; Wilkins, 1967). For this reason, the electrophoretic mobility of nanoparticles was determined in water, phosphate-buffered saline, pH 7.4, and in human blood serum. The results are presented in Table 5. The particle movement was determined optically using a white light or a laser light source. Therefore, the use of nanoparticle aggregates facilitated the observation. As mentioned above, without sonication poly(methyl methacrylate) nanoparticles form aggregates, some of which were visible in the microscope of the electrophoresis cell. Polyacrylamide nanoparticle aggregates from freeze-dried samples are visible only for a few minutes, because these particles disperse easily in

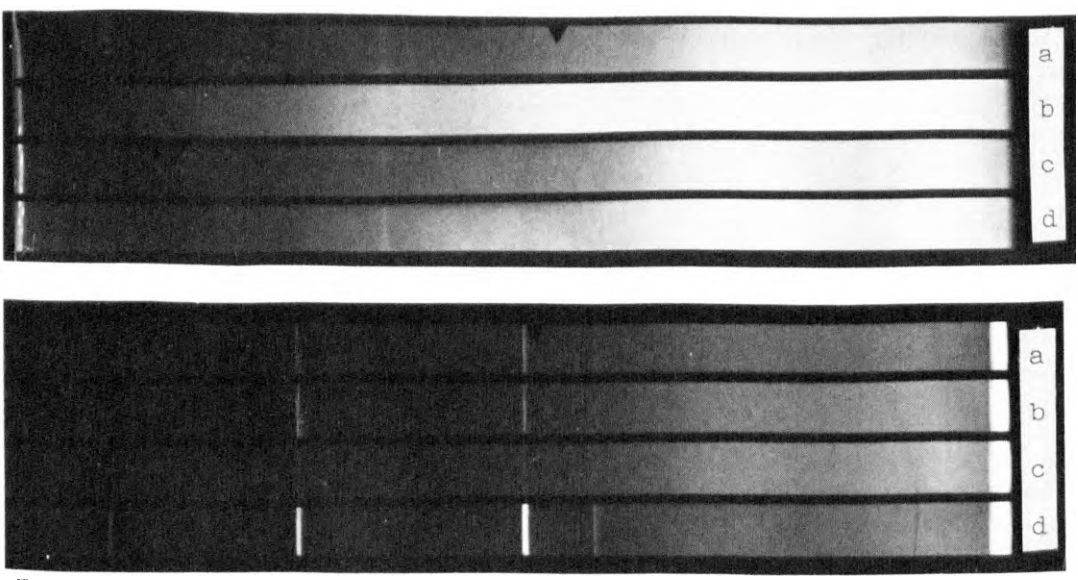

Fig. 11. X-ray diffraction patterns: (a) poly(methyl methacrylate) beads, 10 μm; (b) blank; (c) poly(methyl methacrylate) nanoparticles; (d) polyacrylamide nanoparticles.

Fig. 12. X-ray diffraction patterns: (a) polymethylcyanoacrylate nanoparticles, (b) Polyethylcyanoacrylate nanoparticles, (c) Polybutylcyanoacrylate particles, (d) Sodium chloride. Sodium chloride is present in all of the nanoparticle samples due to the manufacturing method.

TABLE 5

ELECTROPHORETIC MOBILITY ($\mu m \cdot cm \cdot s^{-1} \cdot V^{-1}$) OF NANOPARTICLES (MEAN ± S.D. *)

Polymer	Medium		
	Water	Phosphate-buffered saline, pH 7.4	Human serum
Poly(methyl methacrylate)	-2.76 ± 0.57	-1.30 ± 0.07	-0.25 ± 0.05
Polyacrylamide	< -0.35	–	–
Polymethylcyanoacrylate	-2.33 ± 0.10	-1.64 ± 0.12	-0.23 ± 0.02
Polyethylcyanoacrylate	-2.18 ± 0.16	-1.32 ± 0.16	-0.23 ± 0.02
Polybutylcyanoacrylate	-2.01 ± 0.16	-0.87 ± 0.07	-0.19 ± 0.03

* Standard deviation.

aqueous media. For this reason, the value given in Table 5 is only approximate, and no measurements could be made in phosphate-buffered saline and serum.

Any surfactants present in a sample had to be removed because the surface charge was influenced by the physicochemical properties of any adsorbed materials. The polycyanoacrylate samples used for the determination of the electrophoretic mobility therefore were separated from the surfactants by centrifugation and washed 3 times with water before lyophilization. As mentioned before, this treatment led to the formation of aggregates. These aggregated nanoparticles had the advantage of being very suitable for the electrophoretic mobility measurements.

As shown in Table 5, all nanoparticles were negatively charged. With the exception of phosphate-buffered saline as the dispersion medium, poly(methyl methacrylate) nanoparticles had the highest surface charge. Polycyanoacrylates had a slightly lower charge with a tendency for a decrease in charge with increasing ester side-chain length. Polyacrylamide nanoparticles had a very low surface charge. Phosphate-buffered saline reduced the surface charge significantly in comparison to water. This is of course expected because the surface charge is dependent on the ionic strength. Serum yielded an even more pronounced decrease in surface charge, which is caused by the adsorption of serum contents, demonstrating a significant interaction of these components with the nanoparticles.

Water contact angles

Another parameter that is of great importance for the fate of particulate matter in the blood is the hydrophilicity/hydrophobicity of the particle surface. The latter have a profound influence on the interaction of the particles with blood components (Lindsay et al., 1980; Andreade et al., 1979a and b; Chuang et al., 1979, 1980; Baier and Dutton, 1969; Packham et al., 1969; Baszkin and Lyman, 1980), and this in turn influences the body distribution (Saba, 1970). The hydrophilicity/hydrophobicity can be determined by the measurement of the water contact angle (Andreade et al., 1979a and b). Since the water contact angle can only be measured on plain surfaces, the nanoparticles were compressed to tablets. In the case of the polycyanoacrylates, the particles were centrifuged and washed 3 times with water prior to drying and

TABLE 6

WATER CONTACT ANGLES OF NANOPARTICLES

Polymer	Contact angle [a]	
Poly(methyl methacrylate)	72.7 ± 7.0	$P < 0.1$
Polybutylcyanoacrylate	68.9 ± 10.3	$P < 0.1$
Polyethylcyanoacrylate	64.7 ± 4.2	$P < 0.0005$
Polymethylcyanoacrylate	55.6 ± 6.4	$P < 0.0005$
Polyacrylamide	40.5 ± 7.6	
Poly(methyl methacrylate) after 12 h storage in human serum	52.7 ± 6.4	
Polybutylcyanoacrylate after 12 h storage in human serum	45.4 ± 8.5	

[a] Mean and standard deviation.

compression. Since polybutylcyanoacrylate tablets were too brittle, this material was dissolved in acetone and cast to a film on a glass-slide with subsequent evaporation of the solvent.

In order to investigate the influence of the nanoparticles with blood serum, poly(methyl methacrylate) and polybutylcyanoacrylate nanoparticles were suspended in human serum overnight and after centrifugation and subsequent lyophilization of the nanoparticles also compressed to tablets.

The water contact angles were then determined on the tablet or on the film surface. The data are presented in Table 6.

The water contact angle decreased with decreasing hydrophobicity in the order poly(methyl methacrylate) > polybutylcyanoacrylate > polyethylcyanoacrylate > polymethylcyanoacrylate > polyacrylamide.

Suspension of the nanoparticles in serum caused a considerable decrease of the contact angle of about 20°. This decrease is much more significant than for instance the decrease caused by the chain length effect. This shows that a strong interaction, namely an adsorption of plasma contents on the particle surface, occurred, leading to a strong change in the surface properties.

Acknowledgements

This paper is abstracted in part from a habilitation thesis that is available at the Swiss Federal Institute of Technology's (ETH) main library. The author wishes to thank Dr. Kahr, Inst. f. Grundbau und Bodenmechanik, ETH, Zürich, for the preparation of the X-ray diffraction patterns and for the mercury porosimetry measurements, Dr. M. Müller, Inst. f. Zellbiologie, ETH, Zürich, for the preparation of the transmission electron micrographs, and Mr. Wägli, Inst. f. Festkörperphysik for the preparation of the scanning electron micrographs. The author also wishes to thank Prof. Dr. S.S. Davis, Dept. of Pharmacy, University of Nottingham, for the

opportunity to carry out the electrophoretic mobility and the photon correlation spectroscopy measurements in his department.

References

Andreade, J.D., King, R.N., Gregonis, D.E. and Coleman, D.L., Surface characterization of poly(hydroxyethyl methacrylate) and related polymers. I. Contact angle methods in water. J. Polymer Sci., Polymer Symp., 66 (1979a) 313–366.

Andreade, J.D., Ma, S.M., King, R.N. and Gregonis, D.E., Contact angles at the solid–water interface. J. Colloid Interf. Sci., 72 (1979b) 488–493.

Baier, R.E. and Dutton, R.T., Initial events in interactions of blood with foreign surfaces. J. Biomed. Mater. Res., 3 (1969) 191–206.

Baszkin, A. and Lyman, D.J., The interaction of plasma proteins with polymers. I. Relationship between polymer surface energy and protein adsorption/desorption. J. Biomed. Mater. Res., 14 (1980) 393–403.

Brasseur, F., Couvreur, P., Kante, B., Deckers-Passau, L., Roland, M., Deckers, C. and Speiser, P., Actinomycin D adsorbed on polymethylcyanoacrylate nanoparticles: increased efficiency against an experimental tumor. Eur. J. Cancer; 16 (1980) 1441- 1445.

Birrenbach, G. and Speiser, P.P., Polymerized micelles and their use as adjuvants in immunology. J. Pharm. Sci., 65 (1976) 1763–1766.

Chuang, H., Sharma, N., Mohammad, S. and Mason, R., Adsorption of thrombin onto artificial surfaces and its detection by an immunoradiometric assay. Artif. Organs, 3 Suppl. (1979) 226–232.

Couvreur, P., Kante, B., Roland, M., Guiot, P., Baudhuin, P. and Speiser, P., Polycyanoacrylate nanocapsules as potential lysosomotropic carriers: preparation, morphological and sorptive properties. J. Pharm. Pharmacol., 31 (1979) 331–332.

Keng, E.Y.H., Air and helium pycnometer. Powder Technol., 3 (1969/70) 179–180.

Kopf, H., Charakterisierung, Anwendung und Eignung der Nanokapsulierung auf Acrylamidbasis zur Einhüllung niedermolekularer Arzneistoffe. Diss. ETH Nr. 5458, Zürich, 1975, pp. 61–68.

Kopf, H., Joshi, R.K., Soliva, M. and Speiser, P., Studium der Mizellpolymerisation in Gegenwart niedermolekularer Arzneistoffe. I. Herstellung und Isolierung der Nanopartikel, Restmonomerenbestimmung, physikalisch-chemische Daten. Pharm. Ind., 38 (1976) 281–284.

Kreuter, J. and Liehl, E., Protection induced by inactivated influenza virus vaccines with polymethylmethacrylate adjuvants. Med. Microbiol. Immunol., 165 (1978) 111–117.

Kreuter, J. and Liehl, E., Long-term studies of microencapsulated and adsorbed influenza vaccine nanoparticles. J. Pharm. Sci., 70 (1981) 367–371.

Kreuter, J., Mauler, R., Gruschkau, H. and Speiser, P.P., The use of new polymethylmethacrylate adjuvants for split influenza vaccines. Exp. Cell Biol., 44 (1976) 12–19.

Kreuter, J. and Speiser, P.P., New adjuvants on a polymethylmethacrylate base. Infect. Immunity, 13 (1976) 204–210.

Lindsay, R.M., Mason, R.G., Kim, S.W., Andreade, J.D. and Harkim, R.M., Blood surface interactions. Trans. Amer. Soc. Artif. Intern. Organs, 26 (1980) 603–609.

Mayer, R.P. and Stowe, R.A., Mercury porosimetry—breakthrough pressure for penetration between packed spheres. J. Colloid Sci., 20 (1965) 893–911.

Müller, M., Meister, N. and Moor, H., Freezing in a propane jet and its application in freeze-fracturing. Mikroskopie, 36 (1980) 129–140.

Packham, M.A., Evans, G., Glynn, M.F. and Mustard, J.F., The effect of plasma proteins on the interactions of platelets with glass surfaces. J. Lab. Clin. Med., 73 (1969) 686–697.

Riddle, E.H., Monomeric Acrylic Esters. Reinhold, New York, 1954, p. 15.

Saba, T.M., Physiology and physiopathology of the reticuloendothelial system. Arch. Intern. Med., 126 (1970) 1031–1052.

Tessmar, K., Polymerisation der Ester der Acrylsäure und ihrer Homologen. In Müller, E. (Ed.) Methoden der Organischen Chemie (Houben-Weyl), Vol. XIV/1, G. Thieme Verlag, Stuttgart, 1961, p. 1037.

Toyoshima, K., Properties of polyvinyl alcohol films. In Fitch, C.A. (Ed.), Polyvinyl Alcohol, Properties and Applications, Wiley, London-New York-Sydney-Toronto, 1973, pp. 339–389.

Wilkins, D.J., Interactions of charged colloids with the RES. In Di Luzio, N.R. and Paoletti, R. (Eds.), The Reticuloendothelial System and Artheriosclerosis, Plenum Press, New York, 1967, pp. 25–33.

Wilkins, D.J. and Myers, P.A., Studies on the relationship between the electrophoretic properties of colloids and their blood clearance and organ distribution in the rat. Br. J. Exp. Path., 47 (1966) 568–576.